

Optoelectronic Synapse Using Monolayer MoS₂ Field Effect Transistors

*Molla Manjurul Islam,^{1, 2} Durjoy Dev,^{1, 3} Adithi Krishnaprasad,^{1, 3} Laurene Tetard,^{1, 2} and Tania Roy^{1, 2, 3, 4, *}*

¹*NanoScience Technology Center, University of Central Florida, Orlando FL 32826, USA*

²*Department of Physics, University of Central Florida, Orlando FL 32816, USA*

³*Department of Electrical and Computer Engineering, University of Central Florida, Orlando FL 32816, USA*

⁴*Department of Materials Science and Engineering, University of Central Florida, Orlando FL 32816, USA*

**Corresponding author: tania.roy@ucf.edu*

Supporting Information

S1. CVD growth of large area monolayer MoS₂, material characterization and mobility calculation.

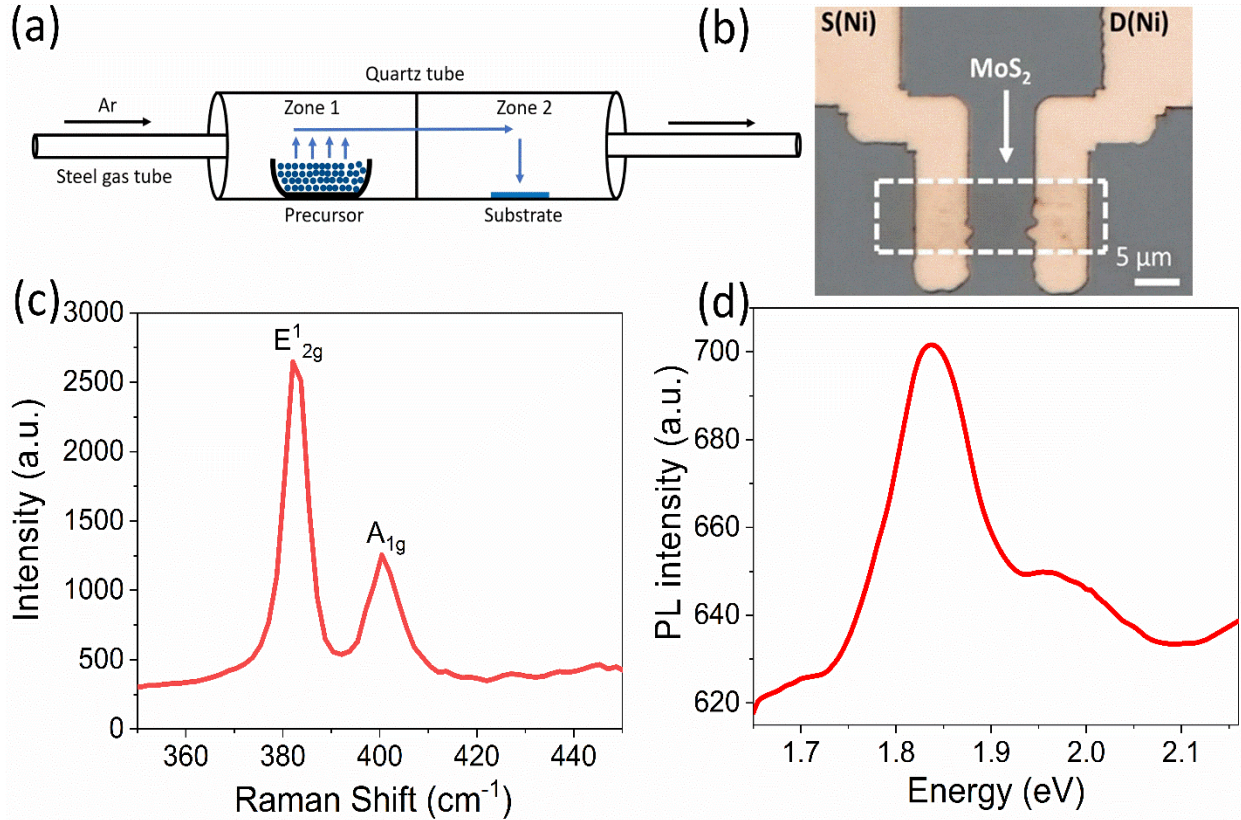


Figure S1. (a) Schematic (not to scale) representation of chemical vapor deposition of monolayer MoS₂. (b) Optical microscopic image of back gated monolayer MoS₂ FET as optoelectronic synapse (c) Raman and (d) PL spectrum of CVD grown monolayer MoS₂.

The typical field effect mobility of the monolayer MoS₂ FET in vacuum is $1.25 \text{ cm}^2 \text{ V}^{-1} \text{ s}^{-1}$, calculated as per the equation $\mu_{FE} = (dI_D/dV_G) (L/W) (1/C_{ox}V_D)$, where μ_{FE} is the field-effect mobility, C_{ox} is the capacitance of the gate oxide, L is the length and W is the width of the conductive channel.

S2. CVD-grown MoS₂ on SiO₂ gate.

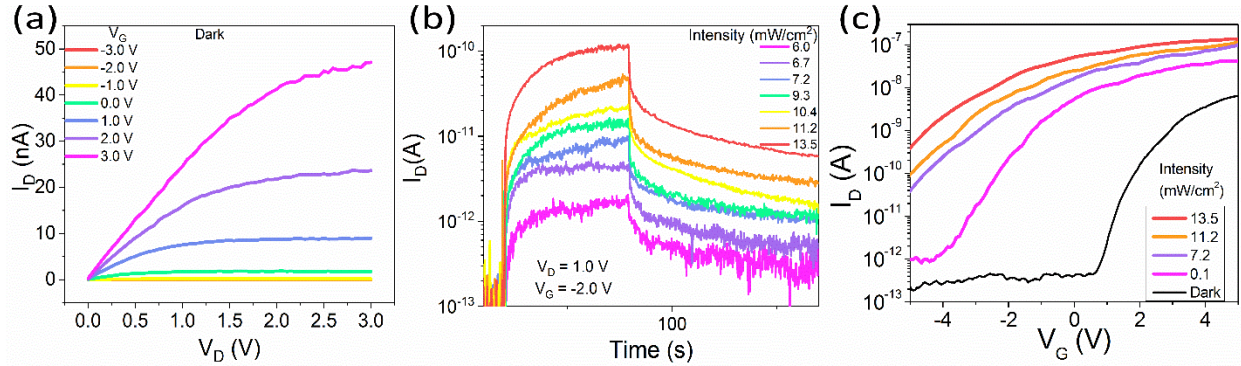


Figure S2. (a) $I_D - V_D$ of CVD grown MoS₂ FET as Optoelectronic Synapse on SiO₂ gate at different V_G in dark. (b) Transient characteristics of the device showing change in the drain current after applying a single light pulse (pulse duration 30 s) with varying intensity at $V_D = 1.0$ V and $V_G = -2.0$ V. (c) $I_D - V_G$ at $V_D = 1.0$ V in dark and with different intensities of incident light.

Figure S2a shows $I_D - V_D$ of CVD grown MoS₂ FET as Optoelectronic Synapse on SiO₂ gate at different V_G in dark. With increasing V_D , the drain current, I_D also increases linearly. The measurement was carried out for gate voltages starting from -3.0 V to 3.0 V. **Figure S2b** represents the transient characteristics of the device showing change in the drain current after applying a single light pulse (on time 30 s) with varying intensity at $V_D = 1.0$ V and $V_G = -2.0$ V. With increasing intensity, drain current, I_D also increases. It signifies the increase in photogenerated carriers. **Figure S2c** shows the $I_D - V_G$ at $V_D = 1.0$ V in dark and with different intensities of incident light, which confirms the photogating effect of the device.

S3. Drain current retention of CVD grown MoS₂ on SiO₂ gate.

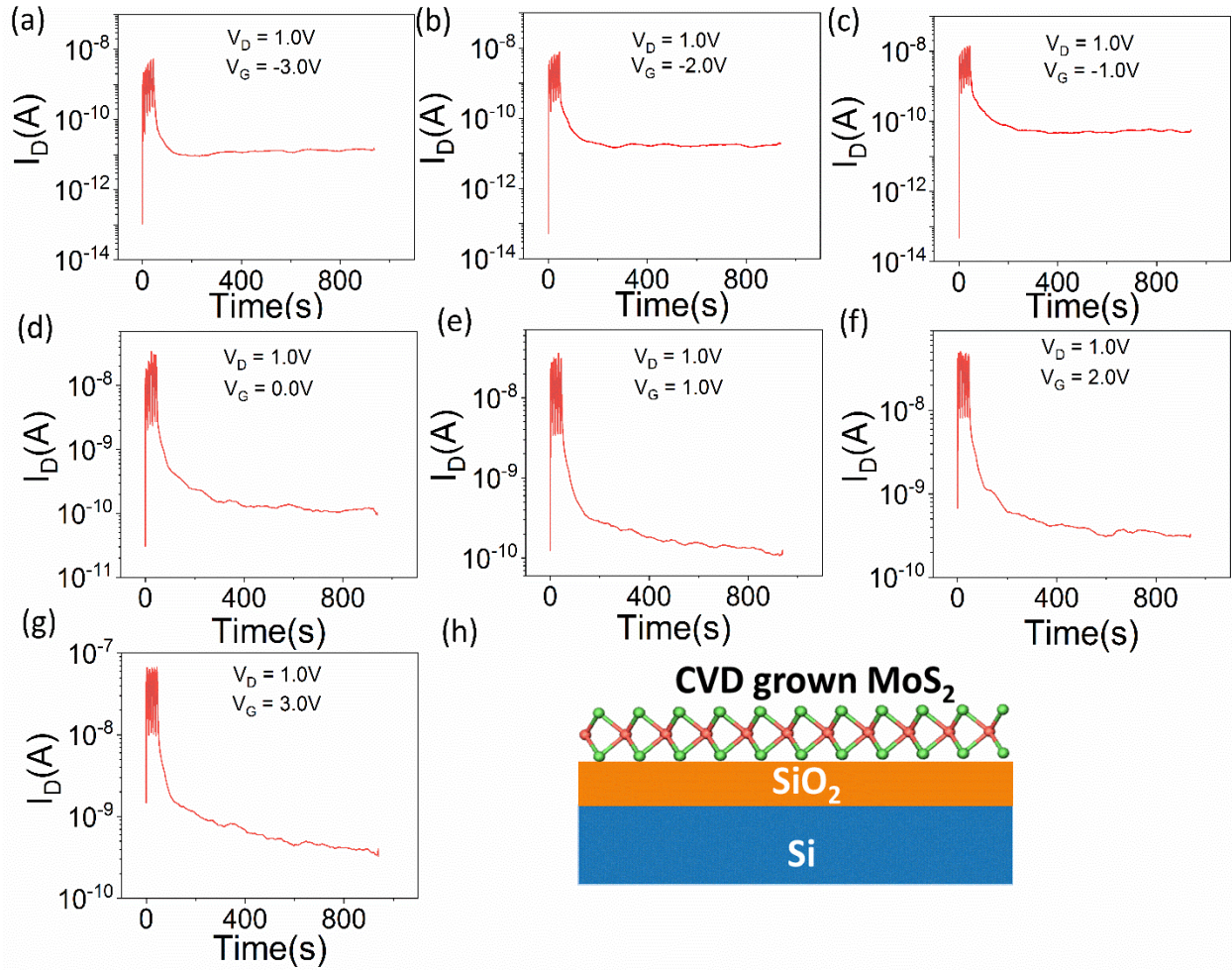


Figure S3. Light stimulated potentiation and drain current retention of CVD grown monolayer MoS₂ on SiO₂ gate at (a) $V_G = -3.0$ V. (b) $V_G = -2.0$ V. (c) $V_G = -1.0$ V. (d) $V_G = 0.0$ V. (e) $V_G = 1.0$ V. (f) $V_G = 2.0$ V. (g) $V_G = 3.0$ V. (h) Schematic diagram of Si/SiO₂/CVD grown MoS₂.

Figure S3 shows the light stimulated potentiation and drain current retention of CVD grown monolayer MoS₂ on SiO₂ gate at different gate voltages. At negative gate voltages, device potentiates with application of each light pulse and retains a huge part of drain current after removing the light source. Device shows maximum retention at $V_G = -1.0$ V.

S4. Drain current retention of CVD grown MoS₂ on Al₂O₃ gate.

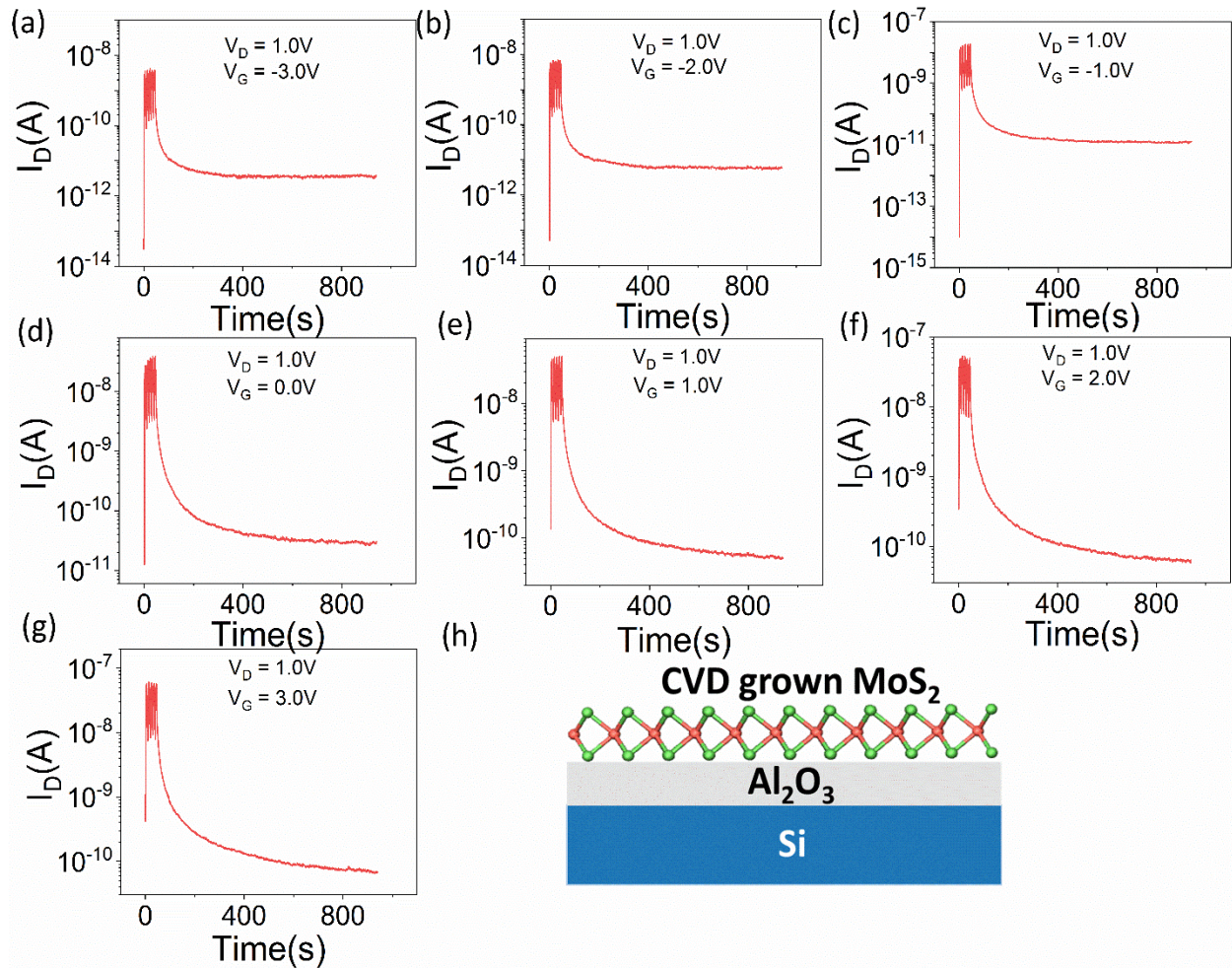


Figure S4. Light stimulated potentiation and drain current retention of CVD grown monolayer MoS₂ on Al₂O₃ gate at (a) $V_G = -3.0$ V. (b) $V_G = -2.0$ V. (c) $V_G = -1.0$ V. (d) $V_G = 0.0$ V. (e) $V_G = 1.0$ V. (f) $V_G = 2.0$ V. (g) $V_G = 3.0$ V. (h) Schematic diagram of Si/Al₂O₃/CVD grown MoS₂.

Figure S4 shows the light stimulated potentiation and drain current retention of CVD grown monolayer MoS₂ on Al₂O₃ gate at different gate voltages. At negative gate voltages, device potentiates with application of each light pulse and retains a huge part of drain current after removing the light source. Device shows maximum retention at $V_G = -1.0$ V. Therefore, device characteristics does not change for replacing SiO₂ gate with Al₂O₃ gate dielectric.

S5. Drain current retention of exfoliated MoS₂ on SiO₂ gate.

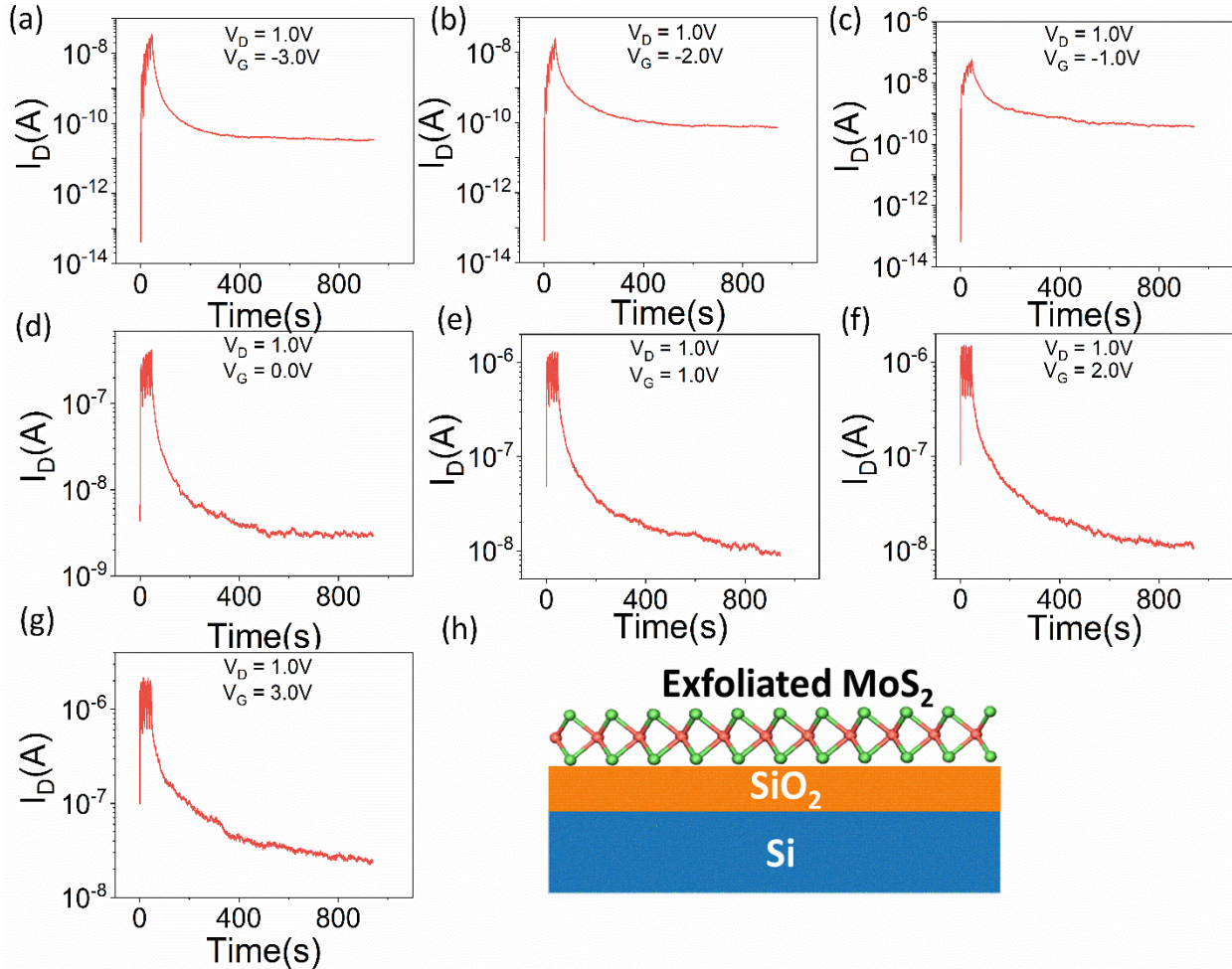


Figure S5. Light stimulated potentiation and drain current retention of exfoliated MoS₂ on SiO₂ gate at (a) $V_G = -3.0$ V. (b) $V_G = -2.0$ V. (c) $V_G = -1.0$ V. (d) $V_G = 0.0$ V. (e) $V_G = 1.0$ V. (f) $V_G = 2.0$ V. (g) $V_G = 3.0$ V. (h) Schematic diagram of Si/SiO₂/Exfoliated MoS₂.

Figure S5 shows the light stimulated potentiation and drain current retention of exfoliated MoS₂ on SiO₂ gate at different gate voltages. At negative gate voltages, device potentiates with application of each light pulse and retains a huge part of drain current after removing the light source. Device shows maximum retention at $V_G = -1.0$ V. Therefore, device characteristics does not change for replacing the CVD grown MoS₂ with exfoliated MoS₂.

S6. $I_D - V_G$, $I_D - V_D$ and drain current retention of exfoliated WSe₂ on SiO₂ gate

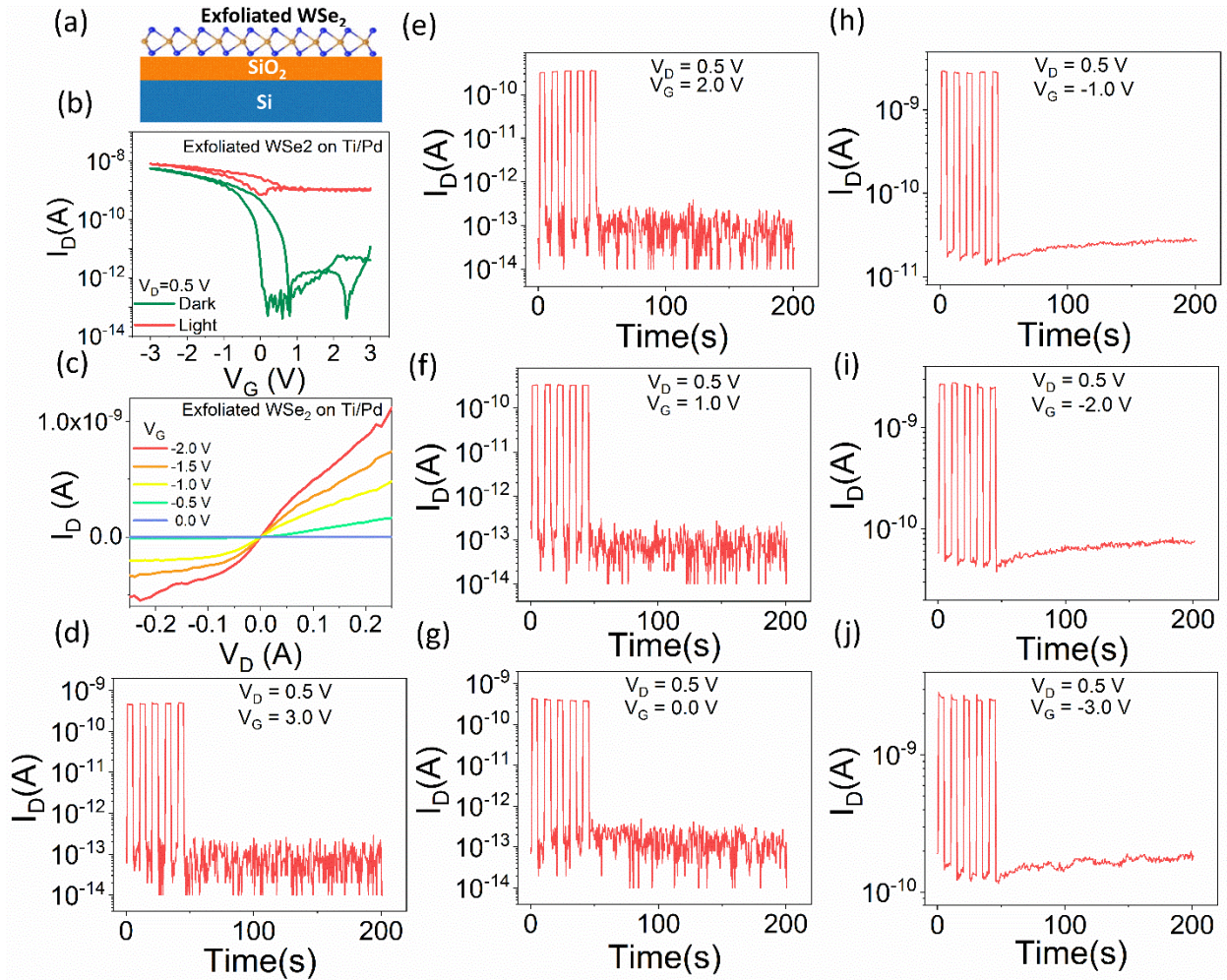


Figure S6. Exfoliated WSe₂ FET on SiO₂ gate: (a) Schematic diagram (b) $I_D - V_G$ at $V_D = 0.5$ V in dark and under light illumination, (c) $I_D - V_D$ at different V_G in dark. Light stimulated potentiation and zero drain current retention of exfoliated WSe₂ on SiO₂ gate at (d) $V_G = 3.0$ V. (e) $V_G = 2.0$ V. (f) $V_G = 1.0$ V. (g) $V_G = 0.0$ V. (h) $V_G = -1.0$ V. (i) $V_G = -2.0$ V. (j) $V_G = -3.0$ V.

Figure S6 shows the exfoliated WSe₂ FET on SiO₂ gate (a) Schematic diagram (b) $I_D - V_G$ at $V_D = 0.5$ V in dark and under light illumination, (c) $I_D - V_D$ at different V_G in dark. Light stimulated potentiation and drain current retention of exfoliated WSe₂ on SiO₂ gate at different gate voltages. Device did not show any retention of drain current for any of the applied gate voltages.

Therefore, WSe₂/MoS₂ interface is not capable of trapping the photogenerated holes. So, the photogenerated carriers recombine as soon as the light source is removed.

S7. Paired pulse facilitation measurement.

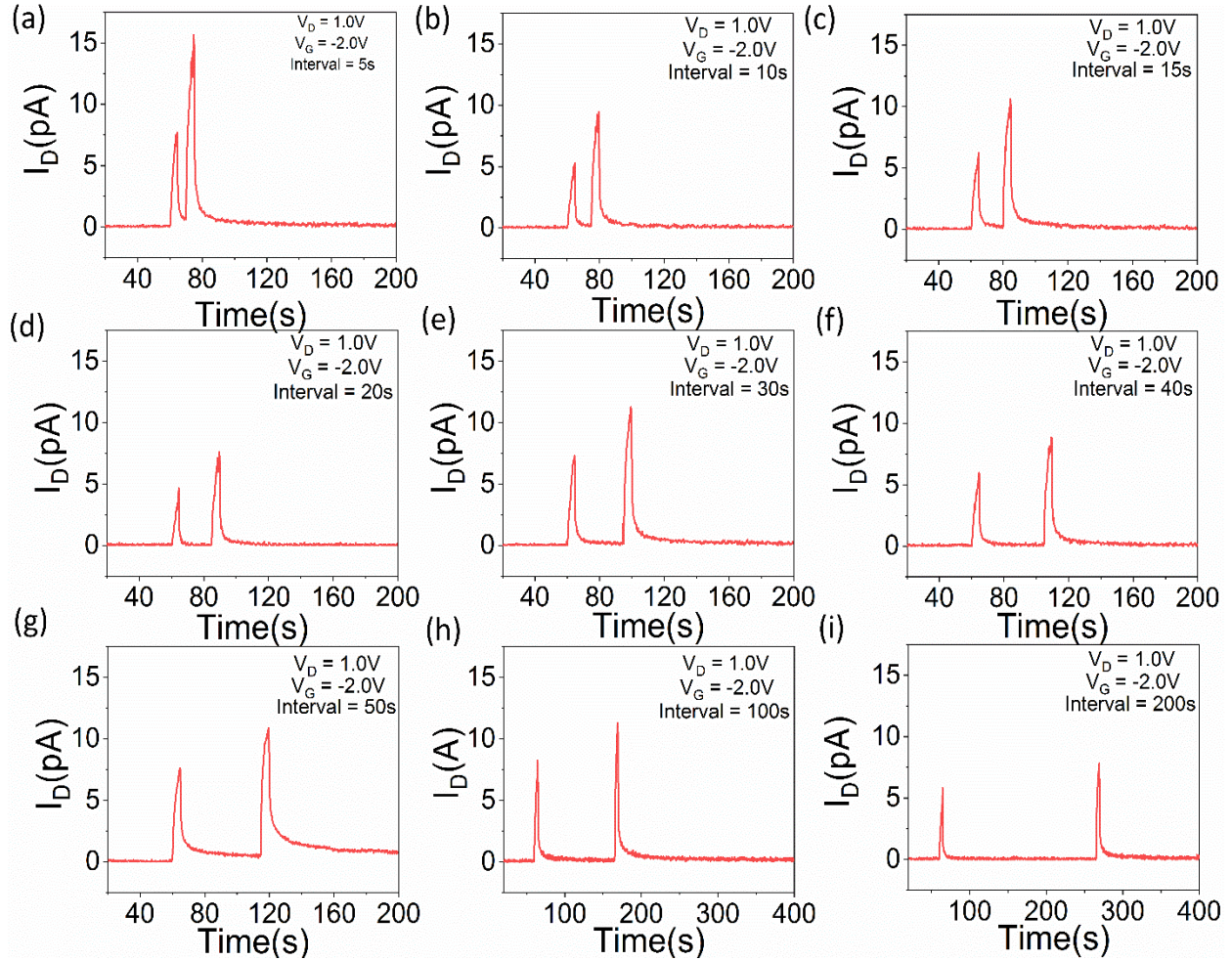


Figure S7. Paired pulse facilitation measurement at $V_D = 1.0$ V and $V_G = -2.0$ V for the time interval (a) 5 s, (b) 10 s, (c) 15 s, (d) 20 s, (e) 30 s, (f) 40 s, (g) 50 s, (h) 100 s, (i) 200 s between two successive light pulses.

Figure S7 shows the paired pulse facilitation measurement at $V_D = 1.0$ V and $V_G = -2.0$ V for different time intervals. Two successive light pulses were applied to the device. With increasing

time difference between the two applied pulses, the drain current amplitude after second pulse decreased gradually. Maximum drain current after second light pulse was recorded for minimum time interval between the two applied pulses.

S8. Spike time dependent plasticity measurement.

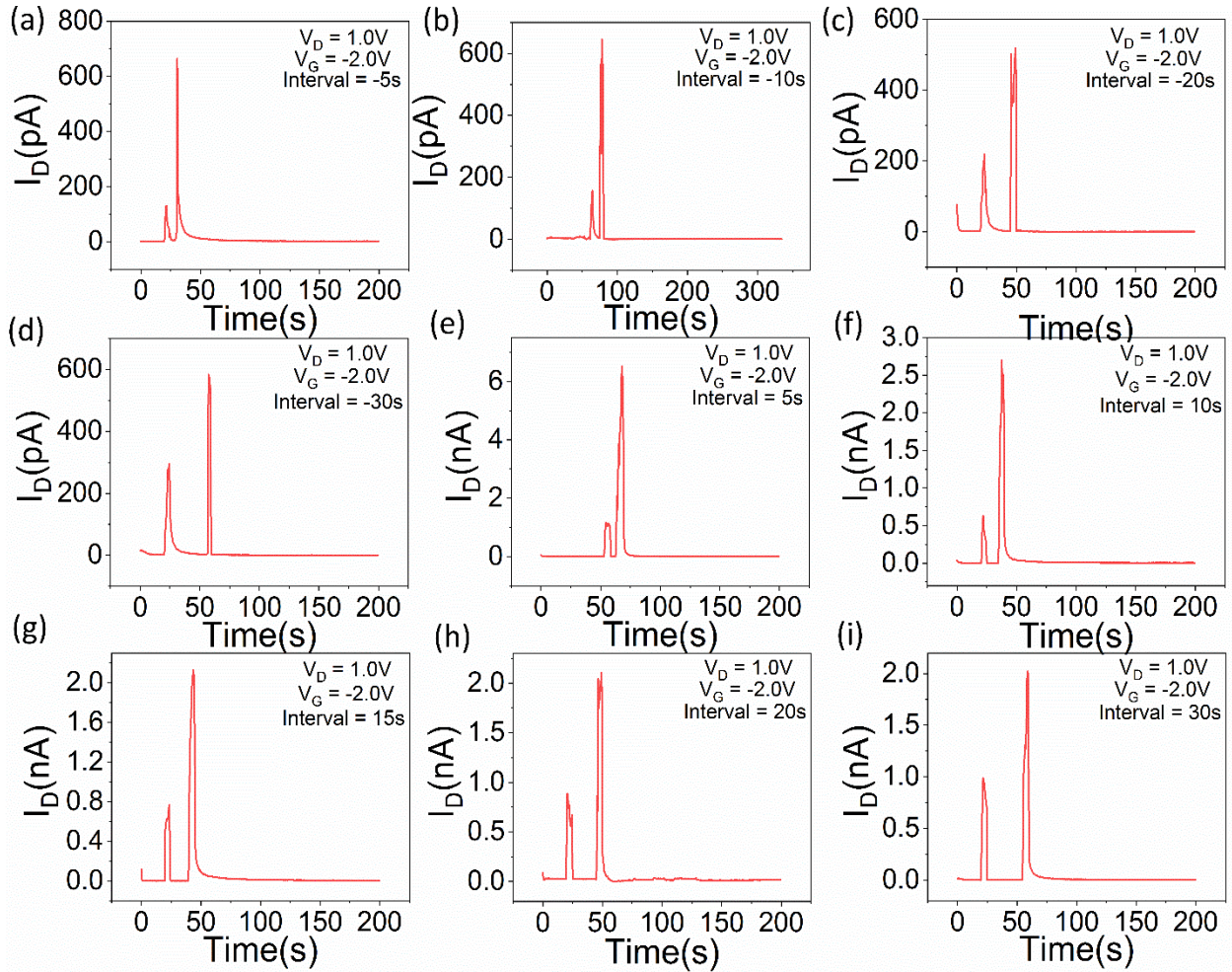


Figure S8. Spike time dependent plasticity measurement at $V_D = 1.0$ V and $V_G = -2.0$ V for the time interval (a) -5 s, (b) -10 s, (c) -20 s, (d) -30 s, (e) 5 s, (f) 10 s, (g) 15 s, (h) 20 s, (i) 30 s between two successive light pulses.

Figure S8 shows the spike time dependent plasticity measurement for different time intervals between two applied light pulses. Two light pulses were applied to two electrically shorted devices separately with a varied time interval at $V_G = -2.0$ V and $V_D = 1.0$ V. With increasing time interval between two applied light pulses, the drain current amplitude after second pulse decreased gradually. When first light pulse was applied on presynaptic device, the time interval was considered positive and when first light pulse was applied on postsynaptic device, the time interval was considered negative.